CP-violating magnetic moments of atoms and molecules

Andrei Derevianko

Department of Physics, University of Nevada, Reno, Nevada 89557, USA

M. G. Kozlov

Petersburg Nuclear Physics Institute, Gatchina 188300, Russia

Abstract

We develop a theory of electric-field-induced magnetization of a medium. The relevant polarizability, β^{CP}, simultaneously violates the inversion symmetry (parity), the time-reversal symmetry, and the combined CP symmetry. We focus on two fundamental mechanisms mediating the appearance of β^{CP} — the electric dipole moment of the electron (eEDM) and the electron-nucleus pseudo-scalar weak neutral currents. Measuring β^{CP} may reveal so-far elusive eEDM and these neutral currents. We start with computing β^{CP} for rare-gas atoms and demonstrate that β^{CP} scales steeply as Z^5 with the nuclear charge Z. Further, we show that β^{CP} manifests itself in permanent CP-violating magnetic moments of molecules. A macroscopic sample of polarized molecules would exhibit a magnetization correlated with the direction of the externally-applied polarizing electric field. We numerically estimate this unconventional moment for diamagnetic molecules. Finally, we introduce a thermally-induced CP-violating magnetization of a sample of paramagnetic molecules. In all cases, we evaluate the feasibility of an experimental search for eEDM. We find that paramagnetic molecules HgH embedded in a rare-gas matrix at a temperature of a few Kelvin have a remarkable sensitivity to eEDM. We conclude, that experiments with such "artificial solids" can push the current limit on the eEDM by several orders of magnitude, deep into the domain of predictions of competing extensions to the Standard Model of elementary particles.

Key words: electron electric dipole moment, weak neutral currents, CP-violation, high-precision magnetometry
PACS: 11.30.Er, 32.80.Ys

Contents

1 Introduction

Much of the progress in understanding fundamental forces in the second half of the 20th century has been guided by the realization that the physics laws do not necessarily remain invariant under discrete symmetry operations: mirror reflection, or parity (P), time (T) reversal, and charge (C) conjugation (particle-antiparticle symmetry). Discovery of parity non-conservation in the nuclear β-decay by Wu et al. (1957) is one of the hallmark discoveries of the 20th century. This discovery has lead to formulation of the theory of electroweak interactions, the cornerstone of the modern Standard Model (SM) of elementary particles. Demise of the parity conservation as the universal law in 1956, was followed in 1964 by the fall of the combined CP symmetry in decays of neutral kaons (Christenson et al. (1964)). This lead to augmenting the SM with the celebrated Cabibbo-Kobayashi-Maskawa quark mixing matrix. Except for this modification and the neutrino oscillations, the SM has been verified in numerous experiments (Amsler et al. (2008)). Yet, the SM is still far from being the ultimate theory of everything: there are several outsinging puzzles, such as the strong force CP problem, the matter-antimatter asymmetry, the hierarchy problem, etc. Contemporary experiments are driven by searches for new physics beyond the Standard Model. The violation of discrete symmetries plays a central role in this quest.

Developments in atomic physics followed those in particle and nuclear physics. Here the ability to carefully listen (high precision), rather than smashing par-

ticles at increasingly higher energies plays a decisive role. At sufficiently high precision, the measurements may become sensitive to virtual contributions of exotic, yet undiscovered elementary particles. The atomic experiments rely on the fact that the Coulomb interactions and the well-established quantum electrodynamics that governs atomic processes are C-, P-, and T- invariant. This allows one to discriminate for otherwise strongly suppressed symmetry-breaking forces. Generally, the low-energy results derived from atomic physics are both unique and complementary to those generated from collider experiments. Commonly, two directions in atomic physics: atomic parity violation (APV) and the search for T,P-violating permanent electric dipole moments (EDM) are considered to be the most fruitful so far.

Rich history of atomic parity violation is examined in a number of review articles, e.g., Bouchiat and Bouchiat (1997); Ginges and Flambaum (2004) and a book by Khriplovich (1991). Here we just briefly touch upon several important milestones. After the discovery of parity violation in nuclear physics, Zel'dovich (1959) contemplated possibility of observing parity-nonconserving signal in atoms. He concluded that the effect was too small to be of experimental significance. In the 1970s, however, Bouchiat and Bouchiat (1974) realized that the APV is amplified in *heavy* atoms. In atomic physics, the first P-violating signal has been observed by Barkov and Zolotorev (1978) in Bi atom. Over the following decades the experiments were refined, with the APV signal observed in several atoms. So far the most accurate measurement has been carried out in ^{133}Cs by Boulder group (Wood et al. (1997)). The latest high-precision atomic-structure analysis (Porsev et al. (2009)) of the Boulder experiment pushed masses of hypothetical extra Z bosons to limits higher than the constraints derived from direct searches with colliders.

In this contribution, we focus on new theoretical developments related to simultaneous violation of P and T symmetries in atomic and molecular physics. One of such violations is related to yet undetected EDMs. Historically, searches for EDMs may be traced back to Purcell and Ramsey (1950); at that time the search was motivated by the fact that EDMs violate parity. After the discovery of parity non-conservation, Landau (1957) pointed out that non-vanishing EDMs would also violate time-reversal. Due to the compelling arguments of the CPT theorem, the T-violation implies CP-violation, a subject of great interest in the physics of fundamental interactions (Bigi and Sanda (2000); Raidal et al. (2008)). While the CP-violation has been discovered in particle physics, the observed amount of violation is not sufficient to explain the imbalance of matter and antimatter in the Universe. One of additional (and tantalizing) motivations is that most supersymmetric extensions of the Standard Model predict electron EDMs (eEDMs) that are within a reach of planned and on-going experimental searches (Fortson et al. (2003)).

A permanent EDM of an atom may arise due to a variety of CP-violating

mechanisms. For example, experiments with diamagnetic (closed-shell) atoms are sensitive to *nuclear* EDMs and nuclear CP-violating interactions: the best nuclear EDM limits are set by experiments with Hg atoms by Griffith et al. (2009). Experiments with paramagnetic (open-shell atoms) are sensitive to *electron* EDM. Namely the eEDM will be the main focus of our present contribution. The current limit on the eEDM,

$$|d_e| < 1.6 \times 10^{-27} e \cdot \mathrm{cm} \,, \qquad (1)$$

is derived from a high-precision measurement by Regan et al. (2002) with a beam of Tl atoms.

In Tl eEDM experiment, one spectroscopically searches for a tiny eEDM-induced splitting of the magnetic sublevels of an atom in an externally applied electric field. Presently, there are several alternative trends in searches for eEDM:

- Employing molecules and molecular ions instead of atoms in spectroscopic experiments (Hudson et al. (2002); Tarbutt et al. (2009); Bickman et al. (2009)).
- Non-spectroscopic solid state experiments (Vasiliev and Kolycheva (1978); Lamoreaux (2002); Baryshevsky (2004); Mukhamedjanov et al. (2003); Heidenreich et al. (2005)).
- Spectroscopy of ultracold atoms in optical traps, lattices, and fountains (Chin et al. (2001); Amini et al. (2007)).
- Non-spectroscopic search with molecules frozen in artificial solids, discussed here.

Here we review a new method for eEDM search (Ravaine et al. (2005); Derevianko and Kozlov (2005); Kozlov and Derevianko (2006)). The method is based on the CP-violating (T,P-odd) magnetic moments and polarizabilities of atoms and molecules.

Central to our consideration will be a relation between macroscopic magnetization $\boldsymbol{M}$ of a substance (gas, solid-state, matrix,...) and applied electric field $\boldsymbol{E}$

$$\boldsymbol{M} = \chi^{CP} \boldsymbol{E}. \qquad (2)$$

As discussed in Section 2, this relation violates both parity and time reversals. The magnetization could be measured using an idealized setup shown in Fig. 1. Microscopically, the magnetization of the ensemble due to external E-field can arise in a number of ways (Section 3.3). In this contribution, we consider three mechanisms:

(1) Microscopic CP-violating (T,P-odd) polarizability β^{CP} of an atom (Section 4). Here a magnetic moment, $\boldsymbol{\mu}$, of an individual atom is induced by the E-field, $\boldsymbol{\mu} = \beta^{CP} \boldsymbol{E}$.
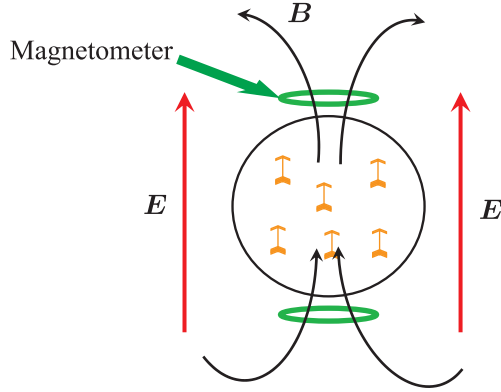
Fig. 1. An idealized scheme for measuring CP-violating (T,P-odd) polarizability of a substance. An external electric field is applied to a sample; unlike the conventional T,P-even electrostatics, the E-field induces macroscopic magnetization. By measuring the resulting magnetic field one could determine the CP-violating polarizability setting a limit on eEDM.

(2) Permanent CP-violating magnetic moment of a diamagnetic molecule (Section 5). In this case, the strong internal molecular E-field, $\boldsymbol{E}_{\mathrm{int}}$, acts on one the atomic constituents and induces the moment $\boldsymbol{\mu}^{CP}$. The resulting CP-violating moment has a definite value in the molecular frame. Then the macroscopic magnetization, Eq.(2), is induced by polarizing a sample of molecules with external E-field.

(3) Thermally-induced magnetic moments of paramagnetic molecules (Section 6). This scheme exploits the link between the EDM of the electron and it's spin, $\boldsymbol{d} = d_e\boldsymbol{\sigma}$, and therefore it's magnetic moment, $\boldsymbol{\mu}_e \approx -\mu_B\boldsymbol{\sigma} = -\mu_B\boldsymbol{d}/d_e$. In an external E-field, because of the coupling of the eEDM to the E-field, thermal populations of the spin-up and spin-down states slightly differ, leading to the magnetization of the sample (Shapiro (1968)). This idea was the basis for solid-state eEDM searches (Vasiliev and Kolycheva (1978); Heidenreich et al. (2005)). Pryor and Wilczek (1987) extended this idea to an "artificial solid": a macroscopic sample of paramagnetic atoms frozen in a matrix of rare-gas atoms. Here we argue that paramagnetic molecules in a matrix have about five orders of magnitude higher sensitivity, than atoms.

In this contribution, we carry out a systematic study of these CP-violating magnetic moments and polarizabilities. We find that the eEDM search with thermally-induced magnetic moments of paramagnetic molecules embedded in a matrix has the largest sensitivity to eEDMs. This scheme combines advantages of solid-state and molecular searches. Indeed, the eEDM effects in molecules are markedly amplified because of the strong internal molecular electric field (Sushkov and Flambaum (1978); Kozlov and Labzowski (1995)), much larger than attainable laboratory fields. In the present solid-state schemes the atomic enhancement of the external electric field for ions of a solid is of the order of unity (Ignashevich (1969); Mukhamedjanov et al.

5

(2003)). By using matrix-isolated diatomic radicals, one can gain up to six orders of magnitude in the effective electric field. At the same time one retains a great statistical sensitivity of the solid-state searches. We show that this particular combination seems to drastically improve sensitivity of the eEDM search. Conservative estimates project that the present limit on eEDM can be improved by several orders of magnitude.

Unless specified otherwise, atomic units $|e| = \hbar = m_e \equiv 1$ and Gaussian system for electro-magnetic equations are used throughout. In these units, the Bohr magneton is $\mu_B = \alpha/2$, where $\alpha \approx 1/137$ is the fine structure constant, and the unit of magnetic field is $m_e^2 e^5/\hbar^4 \approx 1.72 \times 10^7$ Gauss.

2 T, P-violating electrodynamics

We start by reviewing transformation properties of electromagnetic fields and related quantities under the parity and time reversals (see Table 1.) As an illustration, consider the electrostatics, governed by the Gauss and the Ampere's laws. According to the Gauss law, electric field is created by an instantaneous distribution of charges; an inversion of a charge distribution about an arbitrary point in space reverses the direction of the electric field at that point: E-field is a P-odd vector. By contrast, magnetic fields remains unaffected by the charge inversion: B-field is a P-even (axial or pseudo-) vector. Now if we flip the arrow of time (time-reversal), the currents would flow in the opposite directions, while the instantaneous distribution of charges remains the same: apparently, $\boldsymbol{B}$ is a T-odd vector, while $\boldsymbol{E}$ is T-even.

Table 1
Transformational properties of electrodynamic quantities under parity and time reversals.

Quantity	Name	P	T
$\boldsymbol{E}$	Electric field	−	+
$\boldsymbol{B}$	Magnetic field	+	−
ρ	Charge density	+	+
$\boldsymbol{j}$	Current density	−	−
$\boldsymbol{d}$	Dipole moment	−	+
$\boldsymbol{\mu}$	Magnetic moment	+	−
φ	Electric potential	+	+
$\boldsymbol{A}$	Magnetic potential	−	−

The Maxwell equations are invariant under both T and P reversals. For exam-

ple, both sides of the Maxwell-Faraday equation, $\boldsymbol{\nabla} \times \boldsymbol{B} = \boldsymbol{j} + \frac{\partial \boldsymbol{E}}{\partial t}$, transform identically (e.g., the l.h.s. of the equation is P-odd, since the curl operator is P-odd). Notice, however, that the set of four Maxwell equations is incomplete. It has to be supplemented by specifying how individual charges respond to electromagnetic fields. In classical physics this is achieved with the Newton and the Coulomb-Lorentz laws. Since both these laws are P- and T-invariant, these supplementing laws do not spoil the overall symmetry.

2.1 Violation of discrete symmetries and the phenomenology of constitutive relations

Paramount to our consideration is that in more sophisticated theories, the laws that link charge and current densities to driving electromagnetic fields may break the discrete symmetries. Indeed, the parity is broken in the theory of electroweak interactions. To facilitate a phenomenological description of such laws we follow the conventional approach and introduce the macroscopic polarization, $\boldsymbol{P}$, and magnetization, $\boldsymbol{M}$. Relations

$$\boldsymbol{D} = \boldsymbol{E} + 4\pi \, \boldsymbol{P}, \tag{3}$$
$$\boldsymbol{B} = \boldsymbol{H} + 4\pi \, \boldsymbol{M},$$

simply shuffle the effects of bound charges due to $\boldsymbol{P}$ and bound currents caused by magnetization into the definition of the fields.

In the absence of free charges and currents, the Maxwell equations become complete by specifying dependence of $\boldsymbol{P}$ and $\boldsymbol{M}$ on $\boldsymbol{E}$ and $\boldsymbol{H}$ (so-called "constitutive relations").

We start from a linearized local response theory for these relations. In the traditional (T,P-even) electrodynamics,

$$\boldsymbol{P} = \chi_e \boldsymbol{E} \,, \tag{4}$$
$$\boldsymbol{M} = \chi_m \boldsymbol{H} \,, \tag{5}$$

where $\chi_{m,e}$ are the conventionally-defined susceptibilities (true scalars). Notice that both sides of these equations conserve P and T, so that the resulting Maxwell equations remain P- and T-invariant.

To motivate further development, we may, however, also try another linear combination

$$\boldsymbol{P} = \chi^{T,P} \, \boldsymbol{H}, \tag{6}$$
$$\boldsymbol{M} = \chi^{T,P} \, \boldsymbol{E}. \tag{7}$$

These two relations violate both P and T simultaneously, and, therefore, are inadmissible in the traditional electrodynamics. Matching transformational properties of both sides of these equations (reviewed in the upper panel of Table 2) requires that the susceptibility $\chi^{T,P}$ have a pseudo-scalar character and also change sign under the time-reversal. Notice that the very same $\chi^{T,P}$ enters both equations; this symmetry will be addressed in Section 2.1.1.

Table 2
Transformational properties of quantities relevant to phenomenological description of electrodynamics of media with violation of discrete symmetries. The last two columns compile the phases acquired by a given quantity due to parity (P) and time (T) reversals.

Quantity	Name	P	T
$\boldsymbol{D}$	Displacement field	$-$	$+$
$\boldsymbol{H}$	Auxiliary magnetic field	$+$	$-$
$\boldsymbol{P}$	Macroscopic polarization	$-$	$+$
$\boldsymbol{M}$	Macroscopic magnetization	$+$	$-$
$\chi_e,\ \chi_m$	Conventional susceptibilities	$+$	$+$
χ^P	P-odd susceptibility	$-$	$+$
$\chi^{T,P} \equiv \chi^{CP}$	T,P-odd susceptibility	$-$	$-$
χ^T	T-odd susceptibility	$+$	$-$
$\boldsymbol{g}_E,\ \boldsymbol{g}_H$	Conventional gyration vectors	$+$	$+$
$\boldsymbol{g}^P$	P-odd gyration vector	$-$	$-$
$\boldsymbol{g}^{T,P} \equiv \boldsymbol{g}^{CP}$	T,P-odd gyration vector	$-$	$+$
$\boldsymbol{g}^T$	T-odd gyration vector	$+$	$-$

One may proceed with characterizing the substance with all possible scalar, χ, and vector, $\boldsymbol{g}$, quantities which transform in all possible ways under the T and P reversals (there are 10 such quantities, compiled in Table 2). Then we may construct a generalized set of constitutive relations by forming products of electric and magnetic fields with these quantities and requiring that the resulting combinations transform as the $\boldsymbol{D}$ and $\boldsymbol{B}$ fields. Such a set of P-, T-violating local linearized phenomenological relations was proposed by Moskalev (1986). Here, for completeness, we augment the Moscalev's relations with purely T-odd effects.

For static fields,

$$\boldsymbol{D} = (1 + 4\pi\chi_e)\boldsymbol{E} + \chi^{T,P}\boldsymbol{H} - \boldsymbol{g}^P \times \boldsymbol{H}, \tag{8}$$

$$\boldsymbol{B} = (1 + 4\pi\chi_m)\boldsymbol{H} + \chi^{T,P}\boldsymbol{E} + \boldsymbol{g}^P \times \boldsymbol{E}. \tag{9}$$

Apparently, the last terms involving a constant vector $\boldsymbol{g}^P$ describe a non-uniform (gyrotropic) media, characterized by a preferred direction.

For time-dependent fields, the additional terms to the r.h.s. of Eqs. (8,9) are

$$\boldsymbol{D}' = i\boldsymbol{E} \times \boldsymbol{g}_E + \chi^P \, \nabla \times \boldsymbol{E} + \chi^T \, \nabla \times \boldsymbol{H} - \boldsymbol{g}^{T,P} \times (\nabla \times \boldsymbol{E}) + \boldsymbol{g}^T \times (\nabla \times \boldsymbol{H}) \, , \tag{10}$$

$$\boldsymbol{B}' = i\boldsymbol{H} \times \boldsymbol{g}_H + \chi^P \, \nabla \times \boldsymbol{H} + \chi^T \, \nabla \times \boldsymbol{E} + \boldsymbol{g}^{T,P} \times (\nabla \times \boldsymbol{H}) - \boldsymbol{g}^T \times (\nabla \times \boldsymbol{E}) \, . \tag{11}$$

The first term on the r.h.s. of each equation is present in the traditional, T,P-even, electrodynamics: the gyration vector $\boldsymbol{g}_E$ is a real pseudo-vector. The enumerated effects do appear only for the time-dependent cases: according to the Maxwell's equations, for stationary fields and in the absence of free currents, all the curls vanish.

2.1.1 Energy conservation

Insights can be drawn from computing the energy density of the electromagnetic field u. The elementary variation of the energy density is expressed in terms of the fields as (Jackson (1999))

$$\delta u = \frac{1}{4\pi} \left(\boldsymbol{E} \cdot \delta \boldsymbol{D} + \boldsymbol{H} \cdot \delta \boldsymbol{B} \right) .$$

By plugging in Eqs. (8,9) we arrive at

$$u = \frac{1}{8\pi} \left(\varepsilon E^2 + \mu H^2 \right) + \frac{1}{4\pi} \chi^{T,P} \boldsymbol{E} \cdot \boldsymbol{H} + \frac{1}{4\pi} \left(\boldsymbol{E} \times \boldsymbol{H} \right) \cdot \boldsymbol{g}^P .$$

Here the first term comes from the conventional electrodynamics. A particular choice of signs and symmetry of coefficients in Eqs.(8–11) becomes especially transparent if we were to use this energy density as a starting point for a Lagrangian formulation of the Maxwell equations. For example, the second term would contribute equally to both D and B fields, thus we have the very same material coefficient $\chi^{T,P}$ for both cases. The third term contains the cross product, $\boldsymbol{E} \times \boldsymbol{H}$; it is antisymmetric with respect to swapping $\boldsymbol{E}$ and $\boldsymbol{H}$, therefore the relevant contributions to the r.h.s. of Eqs.(8,9) have opposite signs.

To reiterate, we keep the original Maxwell equations; the violations of fundamental symmetries are rather associated with the substance properties (Table 2). In this regard it is important to distinguish between "simulated" and "true" substance effects in violation of fundamental symmetries. For example, the Ohm's law, $\boldsymbol{j} = \sigma \boldsymbol{E}$, violates the time reversal. This violation, however, is related to the second law of thermodynamics (which fixes the direction of the time arrow).

3 Fundamental mechanisms of P and T violation

All mechanism of T,P-violation in atoms necessarily involve either nuclear or electron spin degrees of freedom. In this section, we briefly review fundamental mechanisms of CP violation associated with the electron spin, the focus of our present contribution (see Khriplovich and Lamoreaux (1997) for a discussion of CP violating mechanisms associated with the nuclear spin, such as the Schiff and M2 nuclear moments). There are two possible sources of T and P violation: the permanent EDM of the electron, Sec. 3.1, and the T,P-odd electron-nucleus interaction via neutral currents, Sec. 3.2.

In principle, it is also possible to discuss T- and CP-odd, but P-even interactions. However, such interactions are less natural within the modern field theory as they correspond to the Lagrangians with derivatives. Experimentally such interactions are also less studied. However, Conti and Khriplovich (1992) obtained strong indirect limits on them from the EDM experiments. Possible direct experiments were suggested by Kozlov and Porsev (1989); Baryshevsky and Matsukevich (2002) and realized by Hopkinson and Baird (2002). We will not consider such interactions in the present contribution.

The focus of this work is exclusively on the T,P-odd interactions. To be consistent with our previous work and to emphasize the relation to the important CP violation through the CPT theorem, we will use the superscript CP instead of T,P from now on.

All CP violating interactions in atoms and molecules are described by highly singular relativistic operators and their consistent treatment is possible only within the fully relativistic four-component Dirac formalism. In this formalism, atomic electron orbitals can be written as (Johnson (2007))

$$
u_{n\kappa m}(\boldsymbol{r}) = \frac{1}{r}
\begin{pmatrix}
iP_{n\kappa}(r)\ \Omega_{\kappa m}(\hat{r}) \\
Q_{n\kappa}(r)\ \Omega_{-\kappa m}(\hat{r})
\end{pmatrix},
\tag{12}
$$

where P and Q are the large and small radial components, respectively, and Ω is the spherical spinor. The angular quantum number $\kappa = (l - j)(2j + 1)$. These atomic orbitals will be also used for evaluating the CP-odd effects in molecules; the molecular orbitals will be expanded in terms of (12).

3.1 Permanent electric dipole moment of the electron

In the nonrelativistic approximation an average electric field on the electron in an atom should be zero (because average acceleration on a stationary orbit

is zero). This means that the external E-field is completely screened out by polarization of the electronic cloud. In order to account for this screening, the relativistic interaction of the eEDM with the electric field $\mathcal{E}$ can be written in the following form (Khriplovich (1991)):

$$V^{\text{CP,EDM}} = 2d_e \begin{pmatrix} 0 & 0 \\ 0 & \boldsymbol{\sigma} \cdot \mathcal{E} \end{pmatrix}. \tag{13}$$

This interaction vanishes if we neglect the small component of the bi-spinor (12). Atomic matrix element of this interaction is given by

$$V_{ab}^{\text{CP,EDM}} = d_e \left\{ 2Z \int_0^\infty \frac{dr}{r^2} Q_a(r) Q_b(r) \right\} \delta_{\kappa_a, -\kappa_b} \delta_{m_a, m_b}, \tag{14}$$

where we used the fact that the dominant contribution is accumulated close to the nucleus, so that $\mathcal{E}$ can be approximated by the unscreened nuclear field Z/r^2. Note that if we use the operator (13), the external electric field can be neglected. The selection rules in (14) with respect to the angular quantum numbers m and κ arise because V^{CP} is a pseudoscalar.

3.2 CP-odd neutral currents

It is known that in atomic experiments the effects of eEDM are indistinguishable from those from the scalar CP-odd weak neutral currents. More generally, they lead to the same terms in Eqs. (8–11). Such interactions were discussed since the weak neutral currents were introduced into the electroweak theory. They may be written as (Khriplovich and Lamoreaux (1997))

$$V^{\text{CP,NC}} = \mathrm{i}\frac{G_\text{F}}{\sqrt{2}}(Zk_1^p + Nk_1^n)\gamma_0\gamma_5\rho(\boldsymbol{r}) \equiv \mathrm{i}\frac{G_\text{F}Z}{\sqrt{2}}k_1^{\text{nuc}}\gamma_0\gamma_5\rho(\boldsymbol{r}), \tag{15}$$

where $G_\text{F} = 2.2225 \times 10^{-14}$ a.u. is the Fermi constant, $k_1^{p,n}$ are dimensionless coupling constants of the scalar P,T-odd weak neutral currents for proton and neutron ($k_1^{\text{nuc}} \equiv k_1^p + \frac{N}{Z}k_1^n$). Further, Z and N are the numbers of protons and neutrons in the nucleus, $\gamma_{0,5}$ are the Dirac matrices, and $\rho(\boldsymbol{r})$ is the nuclear density normalized to unity. The presence of $\rho(\boldsymbol{r})$ in Eq. (15) means that the interaction takes place only when the electron is inside the nucleus.

Matrix elements of interactions (13, 15) depend on the short distances and become strongly suppressed with increasing total angular momentum j. To a good approximation, one may neglect all matrix elements involving $j \geq 3/2$. For the remaining matrix elements between orbitals $s_{1/2}$ and $p_{1/2}$ an analytical

expression can be found in Khriplovich (1991):

$$\langle s_{1/2}|V^{\mathrm{CP,EDM}}|p_{1/2}\rangle = \frac{16}{3}\frac{\alpha^2 Z^3 R^{\mathrm{EDM}}}{(\nu_s\nu_p)^{3/2}}d_e, \tag{16}$$

$$\langle s_{1/2}|V^{\mathrm{CP,NC}}|p_{1/2}\rangle = \frac{G_{\mathrm{F}}}{2\sqrt{2}\pi}\frac{\alpha Z^3 R^{\mathrm{NC}}}{(\nu_s\nu_p)^{3/2}}k_1^{\mathrm{nuc}}. \tag{17}$$

Here the effective principal quantum number ν is defined in terms of one-particle energy of atomic electron ε, $\nu = (-2\varepsilon)^{-1/2}$. R^{EDM} and R^{NC} are the relativistic enhancement factors:

$$R^{\mathrm{EDM}} = \frac{3}{\gamma(4\gamma^2-1)} = \begin{cases} 1, & Z=1, \\ 1.4, & Z=54,\ (\mathrm{Xe}), \\ 2.7, & Z=86,\ (\mathrm{Rn}), \end{cases} \tag{18}$$

$$R^{\mathrm{NC}} = \frac{4\gamma(2Zr_{\mathrm{N}})^{2\gamma-2}}{\Gamma^2(2\gamma+1)} = \begin{cases} 1, & Z=1, \\ 2.5, & Z=54, \\ 8.7, & Z=86, \end{cases} \tag{19}$$

where $\gamma = \sqrt{1-(\alpha Z)^2}$ and the radius of the nucleus is taken to be $r_{\mathrm{N}} = 1.2\,(Z+N)^{1/3}\,\mathrm{fm}$.

We see that both CP-odd operators scale as $Z^3\,R$ with the relativistic enhancement factors R given by (18) and (19). Because of the similarity between the matrix elements (16) and (17), there is no need in calculating independently the NC contribution to CP-odd atomic properties. It is sufficient to substitute matrix elements (16) in all the equations with matrix elements (17). This way we find that the contribution induced by the CP-odd weak neutral currents is obtained from the respective eEDM contribution by the following substitution:

$$\frac{d_e}{er_0} \Longleftrightarrow 0.64\times10^{-13}\frac{R^{\mathrm{NC}}}{R^{\mathrm{EDM}}}k_1^{\mathrm{nuc}}, \tag{20}$$

where r_0 is the Bohr radius and R^{EDM} and R^{NC} are given by (18) and (19). The accuracy of Eq. (20) is typically 15 – 20%, which is sufficient for our purposes.

3.3 Microscopic relations

Consider an isotropic medium of weakly interacting quantum species (e.g., atoms and molecules) and express material coefficients introduced in Sec. 2 in terms of their individual properties. For brevity we restrict ourselves to the

case of the static fields. Then we can use Eqs. (8) and (9). For the isotropic medium $\boldsymbol{g}^P = 0$. The remaining three susceptibilities can be written in terms of the operators of the electric and magnetic dipole moments $\boldsymbol{d}$ and $\boldsymbol{\mu}$:

$$\chi_e = \frac{2n}{3} \sum_k \frac{\boldsymbol{d}_{a,k} \cdot \boldsymbol{d}_{k,a}}{E_k - E_a}, \qquad \chi_m = \frac{2n}{3} \sum_k \frac{\boldsymbol{\mu}_{a,k} \cdot \boldsymbol{\mu}_{k,a}}{E_k - E_a}, \tag{21}$$

$$\chi^{CP} = \frac{2n}{3} \Re \sum_k \frac{\boldsymbol{d}_{a,k} \cdot \boldsymbol{\mu}_{k,a}}{E_k - E_a}, \tag{22}$$

where n is the number density. The expressions (21,22) assume that a system is in a fixed quantum state $|a\rangle$; these are to be averaged over thermodynamical distribution over states. Such an averaging will become important for macroscopic samples of molecules, discussed in Sec. 5 and 6.

The relations (21) may be recast into a form involving polarizabilities of the individual species. For example, $\chi_e = n\alpha$, where α is the conventional static electric polarizability. Similarly,

$$\chi^{CP} = n\beta^{CP}. \tag{23}$$

Then the CP-violating magnetic moment of an individual atom will be

$$\boldsymbol{\mu}^{CP} = \beta^{CP} \boldsymbol{E}. \tag{24}$$

All non-chiral species have eigenstates of definite parity P. Operator $\boldsymbol{d} = -e\boldsymbol{r}$ is P-odd and mixes states with different parity. Operator $\boldsymbol{\mu}$ is, on the contrary, P-even and can only mix states with the same parity. Therefore, β^{CP} turns to zero. If we take into account P-odd, T-even interaction between atomic electrons and the nucleus, these selection rules would be broken. However, β^{CP} would still be zero, because a product of matrix elements $\boldsymbol{d}_{a,k}$ and $\boldsymbol{\mu}_{k,a}$ would be purely imaginary. Similar situation takes place in the chiral medium, where parity is not a good quantum number, but the time-reversal symmetry is not violated.

Nonzero polarizability β^{CP} appears only when we include CP-odd interactions V^{CP} from Sec. 3. Then the quantum states are no longer eigenstates of P; moreover, T-reversal symmetry is also broken. In this case, polarizability β^{CP}

in (24) has the form (Ravaine et al. (2005)):

$$\beta^{CP} = \beta_1^{CP} + \beta_2^{CP} + \beta_3^{CP}, \tag{25}$$

$$\beta_1^{CP} = -\frac{2}{3} \sum_{k,l} \frac{V_{a,k}^{\mathrm{CP}} \boldsymbol{\mu}_{k,l} \cdot \boldsymbol{d}_{l,a}}{(E_a - E_k)(E_a - E_l)}, \tag{26}$$

$$\beta_2^{CP} = -\frac{2}{3} \sum_{k,l} \frac{\boldsymbol{\mu}_{a,k} V_{k,l}^{\mathrm{CP}} \cdot \boldsymbol{d}_{l,a}}{(E_a - E_k)(E_a - E_l)}, \tag{27}$$

$$\beta_3^{CP} = -\frac{2}{3} \sum_{k,l} \frac{\boldsymbol{\mu}_{a,k} \cdot \boldsymbol{d}_{k,l} V_{l,a}^{\mathrm{CP}}}{(E_a - E_k)(E_a - E_l)}. \tag{28}$$

4   CP-violating polarizability of diamagnetic atoms

Armed with the general understanding of CP-violating magnetic moments and polarizabilities, now we proceed to systematically analyzing these effects in specific scenarios. In this Section, we treat the simplest case of a closed-shell atom and compute the eEDM-induced CP-violating polarizabilities, (25), of rare-gas atoms He through Rn.

Notice that it is generally assumed that diamagnetic atoms are not useful for the search of the eEDM. A question has been raised by Baryshevsky (2004) if measuring β^{CP} may provide a better route to finding eEDM. To answer this question, we need to carry out computations of this quantity. At the end of this section we estimate sensitivity of the eEDM experiment with liquid Xe (LXe). This experiment appears to be not competitive because of the relatively small signal, but it has an advantage of a low magnetic noise. Another advantage is purely theoretical: here the polarizability β^{CP} may be reliably estimated (Ravaine et al. (2005)). This section will set an important stage for understanding and evaluating CP-violating polarizabilities of molecules and more promising molecular experiments. In particular, we will set up the DHF formalism for computing polarizabilities and prove that β^{CP} scale steeply, as Z^5, with the nuclear charge.

The rest of this section is organized as follows: In Sec. 4.1 we present results of our DHF calculations of β^{CP} for rare-gas atoms. In Sec. 4.2 we derive the Z-scaling of β^{CP}. Finally, in Section 4.3 we evaluate the feasibility of setting a limit on electron EDM by measuring the CP-violating magnetization of liquid Xe.

4.1 Results for rare-gas atoms

Having derived a general third-order expressions for the CP violating polarizability, Eq. (26–28), here we proceed with the atomic-structure part of the evaluation. We employ the conventional Dirac-Hartree-Fock (DHF) or independent-particle approximation for that purpose. In this approach, the atomic many-body wavefunction $|\Psi\rangle$ is represented by the Slater determinant composed of single-particle orbitals (12), which satisfy DHF equation:

$$\left(c(\boldsymbol{\alpha} \cdot \boldsymbol{p}) + \beta c^2 + V_{\text{nuc}} + V_{\text{DHF}}\right) u_i(\boldsymbol{r}) = \varepsilon_i u_i(\boldsymbol{r}), \tag{29}$$

where V_{nuc} is a Coulomb potential of the finite-size nucleus and V_{DHF} is non-local self-consistent DHF potential.

Using a complete set of Slater determinants Eq. (26–28), may be expressed as

$$\beta_1^{CP} = -\frac{2}{3} \sum_{amn} \frac{V_{an}^{\text{CP}} \boldsymbol{\mu}_{nm} \cdot \boldsymbol{d}_{ma}}{(\varepsilon_m - \varepsilon_a)(\varepsilon_n - \varepsilon_a)} + \frac{2}{3} \sum_{abm} \frac{V_{bm}^{\text{CP}} \boldsymbol{\mu}_{ab} \cdot \boldsymbol{d}_{ma}}{(\varepsilon_m - \varepsilon_a)(\varepsilon_m - \varepsilon_b)}, \tag{30a}$$

$$\beta_2^{CP} = -\frac{2}{3} \sum_{amn} \frac{\boldsymbol{\mu}_{an} V_{nm}^{\text{CP}} \cdot \boldsymbol{d}_{ma}}{(\varepsilon_m - \varepsilon_a)(\varepsilon_n - \varepsilon_a)} + \frac{2}{3} \sum_{abm} \frac{\boldsymbol{\mu}_{bm} V_{ab}^{\text{CP}} \cdot \boldsymbol{d}_{ma}}{(\varepsilon_m - \varepsilon_a)(\varepsilon_m - \varepsilon_b)}, \tag{30b}$$

$$\beta_3^{CP} = -\frac{2}{3} \sum_{amn} \frac{\boldsymbol{\mu}_{an} \cdot \boldsymbol{d}_{nm} V_{ma}^{\text{CP}}}{(\varepsilon_m - \varepsilon_a)(\varepsilon_n - \varepsilon_a)} + \frac{2}{3} \sum_{abm} \frac{\boldsymbol{\mu}_{bm} \cdot \boldsymbol{d}_{ab} V_{ma}^{\text{CP}}}{(\varepsilon_m - \varepsilon_a)(\varepsilon_m - \varepsilon_b)}. \tag{30c}$$

Here indexes a and b run over single-particle orbitals occupied in the atomic ground state $|\Psi\rangle$, indexes m and n run over virtual orbitals, and ε_i are the energies of the DHF orbitals.

Equations (30) are now ready for use in calculations with standard atomic codes. They hold for any atomic or molecular system with a state composed from a single Slater determinant. Below we use these for calculations of β^{CP} for the rare-gas atoms. These closed-shell atoms have the $^1S_0$ ground state. The intermediate many-body states in Eq. (26–28) are particle-hole excitations, with the total angular momenta of $J = 0$ or $J = 1$, depending on the multipolarity of the involved operator.

To carry out the numerical evaluation, we solved the DHF equations (29) in the cavity using a B-spline basis set technique by Johnson et al. (1988). The resulting set of basis functions while being finite, may be considered as numerically complete. In a typical calculation, we used a set of basis functions expanded over 100 B-splines. An additional peculiarity related to the Dirac equation is an appearance of negative energy states $(\varepsilon_m < -m_e c^2)$ in the summation over intermediate states in Eq. (30). In our calculations we used the so-called "length form" of the electric-dipole operator and we found the contribution of the negative-energy states to be insignificant.

Table 3

CP-violating polarizability, β^{CP}, in Gaussian atomic units, for rare-gas atoms. CP-violation is either due to the electron EDM, d_e, or due to the neutral currents (15). Notation $x[y]$ stands for $x \times 10^y$.

Atom	Z	β^{CP}/d_e	$\beta^{\mathrm{CP}}/k_1^{\mathrm{nuc}}$
He	2	3.8[−9]	2.4[−22]
Ne	10	2.2[−6]	1.5[−19]
Ar	18	7.4[−5]	5.2[−18]
Kr	36	3.6[−3]	3.1[−16]
Xe	54	4.5[−2]	5.3[−15]
Rn	86	1.07	2.2[−13]

We compute β^{CP}, Eq. (30), using the eEDM-mediated interaction $V^{\mathrm{CP,EDM}}$. The required atomic matrix element is given by Eq. (14). The reduced matrix elements of the magnetic-dipole and electric-dipole moment operators between two bi-spinors are given by

$$\langle a||\mu||b\rangle = \tfrac{1}{2}\left(\kappa_a + \kappa_b\right)\langle-\kappa_a||C_1||\kappa_b\rangle$$
$$\times \int_0^\infty r\,dr\{P_a(r)\,Q_b(r) + Q_a(r)\,P_b(r)\}, \qquad (31)$$

$$\langle a||D||b\rangle = -\langle\kappa_a||C_1||\kappa_b\rangle\int_0^\infty r\,dr\{P_a(r)\,P_b(r) + Q_a(r)\,Q_b(r)\}, \qquad (32)$$

$C_1(\hat{r})$ being normalized spherical harmonic.

Numerical results for rare-gas atoms are presented in Table 3 and also plotted in Fig. 2. In Table 3, the values in the column marked β^{CP}/d_e were computed directly, while the values $\beta^{\mathrm{CP}}/k_1^{\mathrm{nuc}}$ (the last column) were obtained from β^{CP}/d_e using relation (20). From Fig. 2 we observe a pronounced dependence of the polarizability on the nuclear charge Z. Such a steep scaling of the CP-odd polarizabilities is expected from the considerations presented below in Sec. 4.2.

To illustrate the (doubly) relativistic origin of the CP-odd polarizability β^{CP}, we compile values of various contributions to β^{CP} in Table 4 for an isolated Xe atom. Apparently, the dominant contributions are from the two terms in Eq. (30a), but there is strong cancelation between these two terms. As we will see in Sec. 4.2, this cancelation is not accidental.
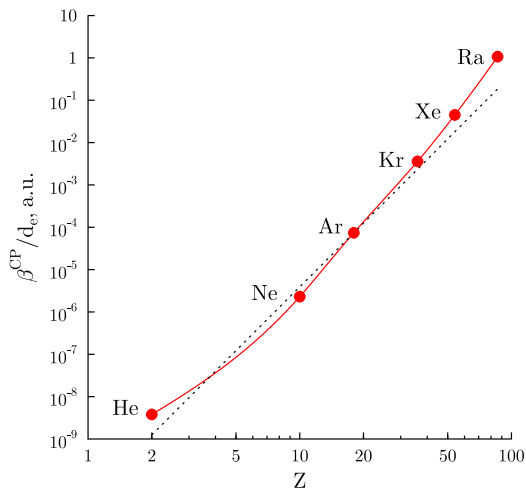
Fig. 2. Dependence of the CP-violating polarizability β^{CP} on the nuclear charge Z for rare-gas atoms. CP-violation is due to the electron EDM, d_e. The ratio β^{CP}/d_e is given in atomic units. The Z^5 line is drawn through Ar value for comparison.

Table 4

Contributions to CP-violating polarizability, β^{CP}/d_e, in Gaussian atomic units, for an isolated Xe atom. CP-violation is due to the electron EDM, d_e. Notation $x[y]$ stands for $x \times 10^y$. Indexes 1 and 2 refer to two terms in each of the equations (30)).

k	Eq.	$\beta^{\mathrm{CP}}_{k,1}/d_e$	$\beta^{\mathrm{CP}}_{k,2}/d_e$	sum
1	(30a)	-0.108	0.132	2.44[−2]
2	(30b)	6.53[−3]	-6.63[−5]	6.46[−3]
3	(30c)	8.19[−3]	5.13[−3]	1.33[−2]
total				4.42[−2]

4.2 Z^5 scaling of β^{CP} for diamagnetic species

Let us consider non-relativistic limit of Eqs. (26 – 28). The one-particle magnetic moment operator is reduced to the form:

$$\boldsymbol{\mu} = \frac{\alpha}{2}(2\boldsymbol{s} + \boldsymbol{l}). \tag{33}$$

This operator can not change electronic principal quantum numbers. Because of that the contributions (27) and (28) vanish, as there $\boldsymbol{\mu}$ should mix occupied and excited orbitals. Thus, we are left with the single term (26), which can be further split in two parts (30a). We will show now that these two contributions cancel each other, as observed from numerical results of Table 4.

17

In the non-relativistic approximation the operator V^{CP} is given by a scalar product of the spin vector and the orbital vector. In the LS-coupling scheme we have following selection rules: $\Delta J = 0$, $\Delta S \leq 1$, and $\Delta L \leq 1$. Therefore, V^{CP} can couple the ground state $^1S_0$ only with excited $^3P_0$ states. Further, the operator $\boldsymbol{\mu}$ (33) is diagonal in the quantum numbers L and S and can couple $^3P_0$ only with $^3P_1$. To return back to the ground state, the dipole operator $\boldsymbol{d}$ has to connect $^3P_1$ with $^1S_0$. However, this matrix element requires a spin flip and vanishes in the non-relativistic approximation. The intermediate states $^3P_{0,1}$ are formed from the excited electron and a hole in the core, which account for two sums in (30a). We conclude that these two contributions must cancel in the non-relativistic approximation.

The matrix element $\langle ^3P_1 | \boldsymbol{d} | ^1S_0 \rangle$ is proportional to the spin-orbit mixing, which is of the order of $(\alpha Z)^2$. It follows from (31) that the relativistic correction to operator (33) is of the same order. This correction accounts for the matrix elements of $\boldsymbol{\mu}$ which are non-diagonal in the principle quantum numbers and leads to the nonzero values of the terms (27) and (28). Thus, we see that all three terms in Eq. (25) are suppressed by the relativistic factor $(\alpha Z)^2$, in agreement with the numerical results from Table 4. The overall scaling of the answer is given by the $\alpha^2 Z^3 R$ scaling of the matrix elements (16,17) and relativistic suppression $(\alpha Z)^2$, i.e., we arrive at the $Z^5 R$ law in agreement with Fig. 2.

4.3   Discussion of experiment with liquid Xe

Consider experimental setup from Fig. 1 to measure the CP-violating polarizability: A strong electric field $\mathcal{E}_0$ is applied to a sample of diamagnetic atoms of number density n. A macroscopic magnetization (7) arises due to the CP-violating atomic polarizability, $\chi^{CP} = n\,\beta^{\mathrm{CP}}$. This magnetization generates a very weak magnetic field B. One could measure this induced magnetic field and set the limits on the electron EDM and on the CP-odd neutral currents. In particular, for a spherical cell, the maximum value of the generated magnetic field at the surface of the sphere can be related to the CP-violating polarizability as

$$B_{\max} = \frac{8\pi}{3} n\,\beta^{\mathrm{CP}} \mathcal{E}_0 \,. \tag{34}$$

Clearly, one should increase the number density to enhance the signal, and it is beneficial to work with a condensed sample (Shapiro (1968)).

Xenon has the most suitable properties for such an experiment among all rare-gas atoms. Xe is the heaviest non-radioactive rare-gas atom; LXe has a large number density ($n \sim 10^{22}\,1/\mathrm{cm}^3$) and a high electric field breakdown strength ($\mathcal{E}_0 \sim 4 \times 10^5 \mathrm{V/cm}$). Our calculations in Section 4.1 were carried out for isolated atoms. However, in a liquid, there are certain environmental

effects (such as confinement of electronic density) that affect the CP-violating signal. To estimate the confinement effects in the liquid, we employ the liquid-cell model. The calculations are similar to those performed by Ravaine and Derevianko (2004). In brief, we solve the DHF equations for a Xe atom in a spherical cavity of radius $R_{\mathrm{cav}} = \left(\frac{3}{4\pi}\frac{1}{n}\right)^{1/3}$, with certain boundary conditions imposed at the cavity surface. For a density of LXe of 500 amagat [1] $R_{\mathrm{cav}} \simeq 4.9$ bohr. For a solid state, $R_{\mathrm{cav}} \simeq 4.2$ bohr and we use the latter in the calculations (see discussion by Ravaine and Derevianko (2004)). Technically, we applied the variational Galerkin method on a set of 100 B-spline functions. We find, that compared to an isolated atom, the CP-violating polarizability of a Xe atom in LXe is reduced by about 65%,

$$\beta^{\mathrm{CP}}(\mathrm{LXe}) \approx 1.5 \times 10^{-2} d_e \,. \tag{35}$$

From Eq. (34) it is clear that the more sensitive the measurement of the B-field, the tighter the constraints on β^{CP} (and d_e) are. Presently, the most sensitive measurement of weak magnetic fields has been carried out by Princeton group (Bui Dang and Romalis (2009)). Using atomic magnetometry, this group has reached the sensitivity level of $2 \times 10^{-12}\,\mathrm{G}/\sqrt{\mathrm{Hz}}$. The projected theoretical limit of this method is $10^{-13}\,\mathrm{G}/\sqrt{\mathrm{Hz}}$ (Kominis et al. (2003)). Notice that this estimate has been carried out for a sample of volume $0.3\,\mathrm{cm}^3$. The sensitivity increases with volume V as $V^{1/3}$, so a $100\,\mathrm{cm}^3$ cell would have sensitivity of about $10^{-14}\,\mathrm{G}/\mathrm{Hz}^{1/2}$. More optimistic estimate, based on nonlinear Faraday effect in atomic vapor (Budker et al. (2000)), is given by Lamoreaux (2002); here the projected sensitivity is $3 \times 10^{-15}\,\mathrm{G}/\sqrt{\mathrm{Hz}}$. For the review of the general trends in modern magnetometry see Budker and Romalis (2007).

Assuming 10 days of averaging, the most optimistic published estimate of the sensitivity to magnetic field (Lamoreaux (2002)) leads to the weakest measurable field of $B \simeq 3 \times 10^{-18}\,\mathrm{G}$. Combining this estimate with the breakdown strength of the E-field for LXe, $\mathcal{E}_0 \sim 4 \times 10^5\,\mathrm{V/cm}$, and our computed value of CP-odd polarizability, Eq. (35), we arrive at the constraint on the electron EDM,

$$d_e(\mathrm{LXe}) < 6 \times 10^{-26}\, e \cdot \mathrm{cm}. \tag{36}$$

This projected limit is more than an order of magnitude worse than the present limit on the electron EDM from the Tl experiment (1). Note, that for the present B-field sensitivity record (Bui Dang and Romalis (2009)), the constraint of electron EDM would be several orders of magnitude weaker.

We conclude, that eEDM experiment with LXe is not competitive. This should not be surprising: as we have seen above, the CP-violating magnetization for diamagnetic LXe is significantly suppressed. In the next section we apply

---

[1] Amagat density unit is equal to 44.615 moles per cubic meter (mol/m^3)

the developed formalism to polar diamagnetic molecules. We will show that, compared to atoms, the molecular CP-violating magnetization is strongly enhanced.

5 CP-violating magnetic moment of diamagnetic molecules

It is a common knowledge, that heteronuclear diatomic molecules have static electric dipole moment aligned with the internuclear axis $\hat{\boldsymbol{n}}$, $\boldsymbol{D} = D\,\hat{\boldsymbol{n}}$. However, there is no similar magnetic moment. An existence of such a magnetic moment would violate both P and T symmetries. Because of the CPT theorem, it would also violate CP symmetry. Thus, we arrive at the permanent molecular CP-violating magnetic moments, $\boldsymbol{\mu}^{\mathrm{CP}} = \mu^{\mathrm{CP}}\hat{\boldsymbol{n}}$, analogous to similar atomic moments considered above. Discussion in this section follows the original paper by Derevianko and Kozlov (2005).

Fig. 3. A strong internal molecular E-field, $\boldsymbol{E}_{\mathrm{int}}$, acts on the heavier atomic constituents and induces the magnetic moment $\boldsymbol{\mu}^{\mathrm{CP}}$. The resulting CP-violating moment has a definite value in the molecular frame.
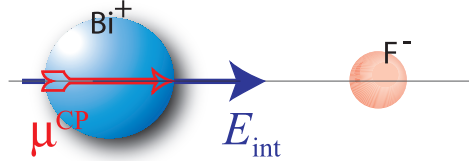
An origin of such a CP-violating magnetic moment becomes qualitatively clear by reverting to the CP-violating polarizability of the previous Section. For the sake of the argument, consider a BiF molecule (see Fig. 3). The chemical bond here is of ionic character, leading to a strong redistribution of charges inside the molecule (the outer-shell electron is stripped off Bi). This charge imbalance generates an enormous E-field, E_{int}, acting on individual atomic constituents. Therefore, according to Sec. 4 each ionic center acquires $\mu^{\mathrm{CP}} = \beta^{\mathrm{CP}} E_{\mathrm{int}}$ (since $\beta^{\mathrm{CP}} \propto Z^5$, μ^{CP} will be dominated by the heavier center). As a result, the molecule acquires the CP-violating magnetic moment. This argument holds for both diatomic and polyatomic molecules.

What is the role of the external electric field in producing the macroscopic magnetization measured in experiment of Fig. 1? The molecular μ^{CP} is fixed in the molecular frame. For a rotating molecule, μ^{CP} would average out to zero in the laboratory frame. An external E-field interacting with the traditional electric-dipole moment of the molecule is needed to align the molecular axes and thus the individual μ^{CP}. Then the macroscopic magnetization will be related to the external field via the now familiar Eq.(2).

The discussed mechanism for generating μ^{CP} is applicable to both diamagnetic

and paramagnetic molecules. However, the regular magnetic moments μ of diamagnetic (closed electronic shells) molecules are strongly suppressed, while for paramagnetic species they are in the order of the Bohr magneton. Notice that the regular $\boldsymbol{\mu}$, however, are not correlated with electric fields and in an experimental setup, Fig. 1, would only lead to a magnetic noise. Clearly, this noise will be smaller for diamagnetic molecules, the subject of this section. We will return to paramagnetic molecules in Sec. 6, where we show that the thermally-induced, rather than the permanent μ^{CP} of this section, become dominant.

At the end of this section we will discuss a possible experiment to search for the CP-violating magnetic moments of heavy polar molecules. We will see that the limit on μ^{CP} derived from such experiments would imply constraints on d_e that are several orders of magnitude better than the values from liquid Xe considered in the previous Section. This is due to the fact that the internal molecular fields are several order of magnitude larger than the attainable laboratory fields.

5.1 Molecular formalism

Diatomic molecule is characterized by the projection $\Omega = (\boldsymbol{J} \cdot \hat{\boldsymbol{n}})$ of the total electronic angular momentum $\boldsymbol{J} = \boldsymbol{L} + \boldsymbol{S}$ on the internuclear axis $\hat{\boldsymbol{n}}$. For a molecular state with a definite Ω, the molecular magnetic moment is directed along $\hat{\boldsymbol{n}}$ and, phenomenologically, we may construct the following combinations of the two vectors

$$\boldsymbol{\mu} = \mu^{\mathrm{CP}}\hat{\boldsymbol{n}} + \mu_B G_{\parallel}\Omega\,\hat{\boldsymbol{n}}, \tag{37}$$

where μ^{CP} and $G_{\parallel}$ are numbers. For the Hund's case (a) G-factor is given by an expression $G_{\parallel}\Omega \approx \Lambda + 2\Sigma$, where $\Lambda = (\boldsymbol{L} \cdot \hat{n})$ and $\Sigma = (\boldsymbol{S} \cdot \hat{n})$ (Landau and Lifshitz (1997)). While the second term in (37) is T,P-even, the $\mu^{\mathrm{CP}}\hat{\boldsymbol{n}}$ term violates both time-reversal and parity. Indeed, under the time reversal the magnetic moment acquires a minus sign, while $\hat{\boldsymbol{n}}$ is T-invariant. Similarly, under parity transformation, $\boldsymbol{\mu}$ is not affected, while $\hat{\boldsymbol{n}}$ flips direction. Thus, the quantum number Ω changes sign under T and P operations.

Given a complete set of molecular states $|k\rangle$ with energies E_k, the magnetic moment μ^{CP} of a state $|0\rangle$ can be computed as

$$\mu^{\mathrm{CP}} = 2\sum_k \frac{\langle 0|\,(\boldsymbol{M} \cdot \hat{\boldsymbol{n}})\,|k\rangle\langle k|V^{\mathrm{CP}}|0\rangle}{E_0 - E_k}\,, \tag{38}$$

where $\boldsymbol{M}$ is the operator of magnetic dipole moment, and the CP-violation is due to interaction V^{CP}. We will focus on eEDM as a source of CP-violation.

In this case V^{CP} is given by Eq. (14). A reanalysis for the CP-odd neutral currents, Eq. (15), can be done in the same way as for atoms using Eq. (20).

The matrix element of V^{CP} depends on short distances from the heaviest nucleus of the molecule (it scales as Z^3). In this matrix element we can neglect screening and put $\boldsymbol{\mathcal{E}}_{\mathrm{int}} \approx (Z/r^2)\,\hat{\boldsymbol{r}}$, where $\boldsymbol{r}$ is the radius-vector of the electron with respect to the nucleus. Below we will evaluate the molecular sum (38) using an approach similar to the LCAO method (linear combination of atomic orbitals).

Note that Eq. (38) is expressed in the body-frame of the molecule. After μ^{CP} is found one has to average Eq. (37) over rotations. In the external electric field $\langle \boldsymbol{n} \rangle \neq 0$ and we get magnetization in the direction of the electric field. The second T,P-even term in Eq. (37) does not contribute to this magnetization. For diamagnetic molecules $(\boldsymbol{J} \cdot \hat{\boldsymbol{n}}) = \Omega = 0$ and this term vanishes. For paramagnetic molecules in the absence of the magnetic field the levels with different signs of Ω are equally populated and this term is averaged to zero.

In this section we are interested in a macroscopic magnetization of a sample of polarized diamagnetic molecules with $\Omega = 0$ due to CP-violating magnetic moments. In this case, the last term in Eq. (37) turns to zero. Some of the molecules may still have non-zero *nuclear* magnetic moments. However, the magnetization due to the nuclear moments is not correlated with polarization of molecules in the external electric field. Moreover, in a macroscopic sample it will effectively average out to zero. Therefore, the magnetic noise in a diamagnetic system is much lower than in paramagnetic one.

To illustrate our qualitative approach to evaluating CP-violating magnetic moments, consider a polar molecule CsF in its ground $^1\Sigma$ state. Halides exhibit a chemical bond of a strong ionic character, and we model the CsF molecule as the Cs^+ ion perturbed by the electric field $\mathcal{E}$ of negative ion F^-. The perturbing field at the Cs^+ is $\mathcal{E} \approx q/R_e^2$, where R_e is the internuclear separation and $q = 1$ is the valency of Cs. The CP-violation is enhanced near the heavier atom and we may evaluate the magnetic moment as

$$\mu^{\mathrm{CP}}(\mathrm{CsF}) \approx \beta^{\mathrm{CP}}(\mathrm{Cs}^+) \frac{q}{R_e^2}, \tag{39}$$

where $\beta^{\mathrm{CP}}(\mathrm{Cs}^+)$ is CP-violating polarizability of the Cs^+ ion. Thus the molecular two-center problem is reduced to computing a one-center property — CP-violating polarizability of the heavier constituent. If both constituents of the diatomic molecule AB have comparable nuclear charges, then $\mu^{\mathrm{CP}}(\mathrm{AB}) \approx [\beta^{\mathrm{CP}}(\mathrm{A}^{(+q)}) + \beta^{\mathrm{CP}}(\mathrm{B}^{(-q)})]\, q R_e^{-2}$, where q is the observed valency of the atoms. In both cases we can calculate molecular moment μ^{CP} using results of Sec. 4.

5.2 Results for polar diatomic molecules

In Table 5 we present numerical results for CP-violating magnetic moments for several diatomics: CsF, BaO, TlF, PbO, and BiF. All these diamagnetic molecules have the $^1\Sigma$ ground state. The heavier atoms of these diatomic pairs are metals, and we assume that the molecules exhibit a pure case of ionic bond, i.e., these heavier atoms fully lend their valence electrons to their electronegative companions (F and O) and become closed-shelled $^1S_0$ ions. The second and third columns of Table 5 list the resulting heavy atomic ions with their nuclear charges, and in the fourth column we present our computed values of CP-violating polarizabilities of these ions. Finally, we combine ionic β^{CP} with the equilibrium internuclear separations (see Eq.(39)) and obtain an estimate for the molecular CP-violating magnetic moments. Our sign convention in expression $\boldsymbol{\mu}^{\mathrm{CP}} = \mu^{\mathrm{CP}}\hat{\boldsymbol{n}}$ is such that the unit vector $\hat{\boldsymbol{n}}$ is directed from the heavier to the lighter nucleus. Notice that we express the μ^{CP} in terms of eEDM. As above, one can use Eq. (20) to relate present results to the strength of the T,P-odd electron-nucleon interaction Eq. (15).

Table 5
Molecular CP-violating magnetic moments, μ^{CP}/d_e, divided by the eEDM for several diamagnetic molecules. The values of μ^{CP}/d_e are dimensionless, d_e and μ^{CP} being expressed in the Gaussian atomic units. The second, third, and the fourth columns list the heavier ion in the molecule, its nuclear charge, and its CP-violating polarizability, β^{CP}/d_e.

Molecule	Ion	Z_{Ion}	$\beta^{\mathrm{CP}}(\mathrm{Ion})/d_e$	μ^{CP}/d_e
CsF	Cs$^+$	55	$-3.0[-2]$	$1.5[-3]$
BaO	Ba^{++}	56	$-2.3[-2]$	$3.4[-3]$
TlF	Tl$^+$	81	$2.9[-1]$	$-1.9[-2]$
PbO	Pb^{++}	82	$3.2[-1]$	$-4.9[-2]$
BiF	Bi$^+$	83	4.8	$-3.2[-1]$

For all the considered molecules, the internuclear separation $R_e \approx 2$Å, and thus the internal molecular fields are comparable. More significant is the effect of increasing CP-violating polarizabilities (the fourth column of Table 5) as one progresses to heavier elements. This trend is largely due to the Z^5 scaling of β^{CP} (see Sec. 4.2). Yet, there is an order of magnitude of difference between β^{CP} for Pb^{++} ($Z = 82$) and Bi$^+$ ($Z = 83$). A part of this large enhancement lies in a softer excitation spectrum of Bi$^+$ and thus smaller energy denominators in Eq. (30). Also, while solving the DHF equations we assumed that the outer shell of Bi$^+$ ion has the $6p^2_{1/2}$ electronic configuration. However, the ground state of Bi$^+$ in a molecule would contain a combination of $6p^2_{1/2}$ and $6p^2_{3/2}$ configurations. Since the $p_{1/2}$ states couple to EDM strongly, while $p_{3/2}$ orbitals

contribute at a much smaller level, we expect that our result for β^{CP} of Bi^+ is somewhat overestimated.

Results of Table 5 should be considered as a qualitative estimate for another reason as well. Expression (39) is based on atomic wavefunctions $|\Phi_i\rangle$, instead of the molecular wavefunctions of the defining expression (38). An underlying assumption is that the molecular wavefunctions $|i\rangle$ in the vicinity of the heavier atomic ion can be expressed perturbatively as

$$|i\rangle \approx \left[|\Phi_i\rangle + \sum_k \frac{\langle \Phi_k| - D_z \mathcal{E} |\Phi_i\rangle}{\varepsilon_i - \varepsilon_k} |\Phi_k\rangle \right] |\Psi_0\rangle \,, \qquad (40)$$

where $|\Psi_0\rangle$ is the wavefunction of the lighter ion (we left out excitations from $|\Psi_0\rangle$ as being non-essential for computing μ^{CP}). Certainly, this model can give only an order of magnitude estimate. For more accurate results the *ab initio* relativistic (!) molecular-structure calculations of CP-violating magnetic moments are necessary.

5.3 *Hypothetical experiment with BiF*

Combining present limit on the eEDM (1) with the computed value of μ^{CP}/d_e for BiF, we obtain:

$$\mu^{\mathrm{CP}}(\mathrm{BiF}) \lesssim 2.4 \times 10^{-37} \mathrm{erg/Gauss} \,. \qquad (41)$$

While this is a remarkably small value, only 2.6×10^{-17} of the electron magnetic moment, measuring such small magnetic moments seems to be possible with the modern magnetometry.

Let us consider a hypothetical experiment, Fig. 1, similar to the one with liquid Xe discussed in Sec. 4.3. Because of rotations, the body-fixed $\boldsymbol{\mu}^{\mathrm{CP}}$ moment averages to zero in the laboratory frame. Experimentally, one needs to apply a polarizing electric field $\mathcal{E}_0$ to orient the molecules along the field. For the efficient polarization of a molecule in its ground rotational state, the coupling to the field must be stronger than the rotational spacing, $D\mathcal{E}_0 > 2B$, where B is the rotational constant. For the ground state of BiF, the rotational constant is $B \approx 0.231 \, \mathrm{cm}^{-1}$, requiring the application of the field $\mathcal{E}_0$ of a few kV/cm. Full polarization of molecules in thermal equilibrium takes place when $D\mathcal{E}_{\mathrm{pol}} > KT$ (Varentsov et al. (1982)). Polarization of a sample of BiF molecules at 10K requires a few tens of kV/cm.

For the experimental setup Fig. 1 and for a fully polarized sample the value of the magnetic field at the surface of the cell in analogy with Eq. (34) is given

24

by

$$B_{\max} = \frac{8\pi}{3} n \, \mu^{\mathrm{CP}} \, . \tag{42}$$

As for all such experiments, the signal is proportional to the number density n of a sample. However, condensing polar molecules with ionic bonds leads to dimerization and subsequent crystallization of the sample. To maintain the individuality of the molecules, one should keep the density sufficiently low, for example, using matrices (see below).

For a qualitative estimate, let us assume the sample number density for BiF to be $10^{21} \, \mathrm{cm}^{-3}$, which is 10 times lower than the density of liquid Xe. If we take μ^{CP} from Eq. (41), which is derived from the present limit on eEDM, from Eq.(42) we obtain a generated B-field of $\mathcal{B} \simeq 2 \times 10^{-15}$ Gauss. Such field can be measured within 20 days of integration time at the present best sensitivity limit of $2 \times 10^{-12} \, \mathrm{G}/\sqrt{\mathrm{Hz}}$ (Bui Dang and Romalis (2009)).

Comparing this estimate with Eq. (36) for the liquid Xe, we find that molecular experiment has a substantially better sensitivity to eEDM. This enhancement is due to (i) larger nuclear charge of Bi ($Z = 83$) than that of Xe ($Z = 54$) and (ii) much larger E-field applied to heavy atom/ion: in case of BiF, the internal molecular field is $\sim 4 \times 10^8 \, \mathrm{V/cm}$, while in liquid Xe the E-field is limited by the breakdown strength of $4 \times 10^5 \, \mathrm{V/cm}$. This large difference in the maximum attainable laboratory field and the internal molecular field (Sandars (1967); Sushkov and Flambaum (1978)) is exploited in more conventional searches for EDMs with molecules by Cho et al. (1989); Tarbutt et al. (2009); Bickman et al. (2009). By contrast to this, all ongoing, or planned eEDM experiments with solids do not use this enhancement (Lamoreaux (2002); Mukhamedjanov et al. (2003); Heidenreich et al. (2005); Sushkov et al. (2009)).

Let us return to the question how to obtain high density sample of polar molecules without dimerization and crystallization. One of the methods to study individual molecules is to use the low-temperature matrices of rare-gas atoms with molecules embedded inside the matrix (Andrews and Moskovits (1989)). The matrix isolation is a well established technique in chemical physics. For chemically stable molecules, the number of guest molecules per host atom (matrix ratio), could be as high as 1/10, i.e., one could attain the number densities of molecules in the order of $10^{21} \, \mathrm{cm}^{-3}$. However, the rare-gas matrix is stable only as a thin layer on a surface of a solid substrate (typical thickness is about $0.1 - 1$ mm). This will lead to the geometrical suppression of the magnetic field, compared to the spherical sample, considered above, and will also reduce signal to noise ratio. On the other hand, matrix isolation technique allows to work with paramagnetic molecular radicals as well, as with diamagnetic stable molecules. As we will see in the next section, paramagnetic molecules provide much stronger CP-violating magnetization and significantly improve potential of the discussed experiments. Therefore, we postpone the

discussion of a more realistic experiment until the end of Sec. 6.

6 Thermally-induced CP-violating magnetization of paramagnetic molecules

In this section we focus on molecular radicals (i.e., molecules with unpaired electron) in the ground $^2\Sigma_{1/2}$ state. We consider a sample of radicals in thermodynamic equilibrium at temperature T. Because of the eEDM coupling to the internal molecular E-field, molecular states with different signs of Ω have slightly different energies. This mechanism leads to a thermodynamically averaged CP-violating (P,T-odd) magnetic moment in molecular body-frame:

$$\langle\mu^{\mathrm{CP}}\rangle = \mu_B\, d_e E_{\mathrm{eff}}/(k_B T)\,, \tag{43}$$

where E_{eff} is the large molecular effective electric field acting on the EDM of the unpaired electron. For paramagnetic molecules E_{eff} grows $\propto Z^3$ with the nuclear charge Z of the heavier molecular constituent (Sandars (1965); Flambaum (1976)) and one would choose to work with heavy radicals. Such molecules as BaF, YbF, and HgH belong to this broad category. Their parameters are summarized in Table 6. Below we will see, that the mercury hydride (HgH) is most suitable for the proposed experiment. For the HgH molecule $E_{\mathrm{eff}} \approx 8 \times 10^{10}\,\mathrm{V/cm}$ and its ESR spectrum in Ar matrix has been studied by Stowe and Knight Jr. (2002).

Table 6
Parameters of several heavy molecules with the ground state $^2\Sigma_{1/2}$. Molecular dipole moments D were measured by Ernst et al. (1986); Sauer et al. (1995); Nedelec et al. (1989). The effective electric field E_{eff} for BaF and YbF was calculated by Kozlov and Labzowski (1995); Titov et al. (1996); Kozlov (1997); Nayak and Chaudhuri (2008). For HgH we rescale results of Kozlov (1985) using relation similar to Eq. (20). Last three columns present polarization $\langle n_z \rangle$, the maximal number density n_{max}, and the accumulation time t_{acc} required to reach S/N=1 for the current limit on eEDM (1). These parameters are calculated with the help of Eqs. (50), (47), and (55) for $E = 10$ kV/cm, $T = 1$K, and sample volume 0.1 cm^3.

Molecule	E_{eff} $\left(10^9 \frac{\mathrm{V}}{\mathrm{cm}}\right)$	D (D)	$\langle n_z \rangle$	n_{max} $\left(10^{20}\frac{1}{\mathrm{cm}^3}\right)$	t_{acc} (ms)
BaF	8	3.17	0.13	0.03	300
YbF	26	3.91	0.16	0.02	30
HgH	79	0.47	0.02	1.5	3

CP-violating moment (43) in analogy with Eq. (38) is directed along internal molecular field and, therefore, along the molecular axis $\hat{\boldsymbol{n}}$. However, there

is important difference between diamagnetic and paramagnetic molecules: instead of electronic denominator in Eq. (38) now we have thermal energy $k_B T$! This results in a huge enhancement of the effect.

For a randomly oriented sample, however, the net magnetization would vanish. When an external E-field is applied, it couples to the traditional molecular electric-dipole moment D and orients the molecules. Taking into account molecular polarization, the CP-moment can be expressed as

$$\langle \mu_{\text{mol}}^{\text{CP}} \rangle \approx \mu_B \frac{d_e E_{\text{eff}}}{k_B T} \times \langle n_z \rangle \,, \tag{44}$$

where $\langle n_z \rangle$ is the average projection of the molecular axis onto the E-field (the field is directed along z-axis). Now the sample acquires a macroscopic magnetization. This magnetization generates an ultraweak magnetic field B^{CP} proportional to eEDM

$$B^{\text{CP}} = 4\pi \gamma \, n \, \langle \mu_{\text{mol}}^{\text{CP}} \rangle \,, \tag{45}$$

where n is the molecular number density and γ is a geometry-dependent factor. For example, near the center of a disk-shaped sample of radius R and thickness L,

$$\gamma = L/2R \,, \tag{46}$$

and near the surface of a spherical sample $\gamma = \frac{2}{3}$ (see Eq. (42)).

Orientation of B-field (45) is linked to that of the applied E-field through $\langle n_z \rangle$ in Eq. (44). Such a link is forbidden in the traditional electrodynamics. Its very presence is a manifestation of the parity and time-reversal violation. By measuring B^{CP} one constrains eEDM via Eqs. (44) and (45). Again we are interested in maximizing density n. However, bringing radicals together is problematic — they react chemically. Here is where the matrix isolation technique becomes key (Andrews and Moskovits (1989)). In this well-established method, the molecules are co-deposited with rare-gas atoms or other species onto a cold ($T \sim 1\,\text{K}$) substrate and become trapped in the matrix (see Fig. 4). Small trapped molecules exhibit properties similar to those for free molecules and a variety of studies, including determination of hyperfine-structure constants has been carried out.

There is an upper limit on the density of trapped molecules; to avoid alignment in the subsystem of guest molecules one requires that thermal agitations are stronger than dipole-dipole interactions between the molecules. We can estimate the maximum density as:

$$n_{\text{max}} \approx \frac{3}{4\pi} \frac{k_B T}{D^2}. \tag{47}$$

A particular advantage of HgH is that its dipole moment is relatively small, $D = 0.47\,\text{Debye}$ (Nedelec et al. (1989)) and at $T = 1\,\text{K}$, the density $n_{\text{max}} \approx 1.5 \times 10^{20}\,\text{cm}^{-3}$.
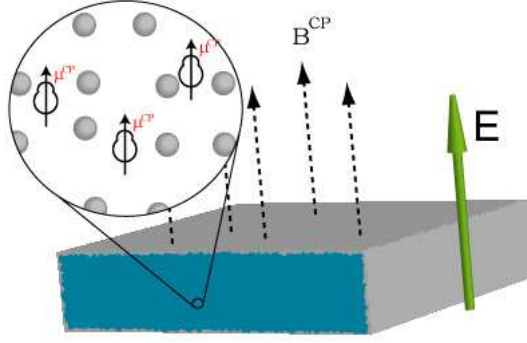
Fig. 4. Scheme of searching for EDM of electron with diatomic radicals embedded in a matrix of rare-gas atoms. A polarizing electric field E is applied to the matrix. As a result, molecular CP-violating magnetic moments μ^{CP} become oriented and generate ultraweak magnetic field B^{CP}.

Estimate (47) agrees with experimental observations that 1:100 guest to host ratio is possible. According to Knight and Sheridan (private communication) the realistic matrix thickness and area are $L = 1$ mm and $S = 1$ cm^2. That corresponds to $\gamma \approx 0.1$ in (45). Recently developed low density plasma beam source (Ryabov et al. (2006)) produces permanent beam of heavy radicals with intensity $\sim 10^{18}$ mol/sterad/s. Placing 1 cm^2 target at 20 cm from the source, one can accumulate necessary number of radicals, i.e. 10^{19}, in 1 hour.

How are the relevant molecular properties modified by the matrix environment? A free non-rotating molecule may be described by the electronic wave function $|\Omega\rangle$, with $\Omega = \pm 1/2$ characterizing projection of spin onto molecular axis. The time-reversal operation T converts Ω-states into each other: $|\Omega\rangle \xrightarrow{T} |-\Omega\rangle$. In the matrix, a molecule can be considered as an individual entity perturbed by the host atoms. The local symmetry of the perturbing fields depends on the position of the molecule in the matrix. Independent of the spatial symmetry the time-reversal symmetry remains. According to the Kramers' theorem, in the absence of magnetic fields, all levels of diatomics with half-integer spin remain two-fold degenerate for any possible electric field.

EDM interaction operates at short distances near the heavier nucleus. Expanding the electronic wavefunction in partial waves we notice that contribution to the eEDM signal of total angular momenta beyond $s_{1/2}-$ and $p_{1/2}-$waves are strongly suppressed because of the growing centrifugal barrier and properties of the eEDM (see Sec. 3). The truncated wave function has the $C_{\infty,v}$ symmetry and Ω still remains a good quantum number for the degenerate states of matrix-isolated radicals. Within this approximation, the effective molecular Hamiltonian in the external field E reads

$$H_{\text{eff}} = -\boldsymbol{D} \cdot \boldsymbol{E^*} + 2d_e E_{\text{eff}} \Omega \,, \tag{48}$$

where E^* is microscopic E-field; for small fields $E^* = E/\varepsilon$. We used H_{eff} to

arrive at Eq. (44).

Using the estimate (44) with the present limit on eEDM (1), we obtain for the thermally-induced CP-odd magnetic moment of HgH molecule trapped at $T = 1\,\mathrm{K}$

$$\langle \mu_{\mathrm{mol}}^{\mathrm{CP}}(\mathrm{HgH}) \rangle < 1.4 \times 10^{-12} \langle n_z \rangle \mu_B \,. \tag{49}$$

Comparing this value with Eq. (41) for BiF we see, that thermally induced CP-violating moment of paramagnetic molecule is about 5 orders of magnitude larger, than that of a diamagnetic molecule with similar Z!

An important parameter entering $\langle \mu_{\mathrm{mol}}^{\mathrm{CP}} \rangle$ is the degree of molecular polarization $\langle n_z \rangle$ in the external E-field. Free diatomic molecules can be easily polarized by the laboratory fields $\sim 10^4 \mathrm{V/cm}$, but there is a paucity of data on polarizing matrix-isolated molecules (Kiljunen et al. (2005)). Certainly, the rotational dynamics of the guest molecule is strongly affected by the matrix cage. The molecular axis evolves in a complex multi-valley potential, subject to the symmetry imposed on the molecules by the matrix cage. Depending on the barrier height between different spatially oriented valleys, the guest molecule may either execute hindered rotation or librations about the valley minima. Khriachtchev et al. (2005) report evidence for hindered rotation of HXeBr and Weltner, Jr. (1990) suggests that other hydrides can rotate. Note also, that for Ar matrix the cell size is 4.5Å, while internuclear distance for HgH is only 1.7Å. That gives us a confidence that the HgH radical can be polarized by the external electric field.

We will distinguish between two limiting cases of molecular polarization: strong and weak fields. In the former limit $\langle n_z \rangle \sim 1$, and in the latter,

$$\langle n_z \rangle = \frac{1}{Z} \sum_{n_z} n_z \exp\left(\frac{DE^* n_z}{k_B T} \right) \approx \frac{DE^*}{k_B T} \langle n_z^2 \rangle. \tag{50}$$

For isotropic orientational distribution, characteristic for the polycrystalline matrixes, $\langle n_z^2 \rangle = 1/3$, and we get

$$\langle \mu_{\mathrm{mol}}^{\mathrm{CP}} \rangle \approx \frac{1}{3} \mu_B \frac{DE^*}{k_B T} \frac{E_{\mathrm{eff}} d_e}{k_B T} \,. \tag{51}$$

The dielectric constant of the rare-gas matrix is close to unity, but addition of polar molecules results in

$$\varepsilon \approx 1 + 4\pi n\alpha = 1 + 4\pi n \frac{D^2 \langle n_z^2 \rangle}{k_B T} \approx 1 + \frac{4\pi}{3} n \frac{D^2}{k_B T}, \tag{52}$$

where α is molecular polarizability. For maximum density (47), $\varepsilon \approx 2$ and $E^* \approx E/2$.

The parameter differentiating the weak- and the high-field regimes is the ratio

DE^*/k_BT. For HgH trapped at $T = 1$ K, the transition occurs at $E^* \approx 100$ kV/cm. The breakdown fields for the rare-gas matrices are unknown, we only notice that for liquid Xe it is 400 kV/cm so that both weak- and high-field regimes may be possibly realized. The moderate $E = 10$ kV/cm field corresponds to $\langle n_z \rangle \approx 0.02$.

Finally, we proceed to evaluating the sensitivity of the proposed eEDM search. There are two crucial criteria to consider: weakest measurable B-field and signal-to-noise ratio. Presently, the most sensitive measurement of magnetic fields has been carried out by the Princeton group (see Kominis et al. (2003) and references therein). This group has reached the sensitivity level of 5.4×10^{-12} G/$\sqrt{\text{Hz}}$. A projected experimental sensitivity of 3×10^{-15} G/$\sqrt{\text{Hz}}$ is published in Lamoreaux (2002). We find that for $\langle n_z \rangle \sim 1$ and for $\gamma = 0.1$ the present eEDM limit may be recovered within integration time of $t = 5$ s for the demonstrated sensitivity and within 10^{-6} s for the projected sensitivity. Alternatively, during a week-long measurement, the present eEDM limit may be improved by 3×10^2 for the demonstrated and by 6×10^5 for the projected B-field sensitivity. These values are reduced by a factor of 50 for a moderate 10 kV/cm polarizing field.

In addition to limitations imposed by the weakest measurable B-field one must also consider signal-to-noise ratio Budker et al. (2006). As we pointed out above, the thermally-induced $\langle \mu_{\text{mol}}^{\text{CP}} \rangle$ of radicals is many orders larger than permanent $\mu_{\text{mol}}^{\text{CP}}$ of diamagnetic molecules discussed in Sec. 5. The magnetic noise from paramagnetic radicals is also much higher as they have traditional magnetic moments associated with unpaired electron spin,

$$\langle \mu_{\text{mol}} \rangle = 2\mu_B \Omega \langle n_z \rangle. \tag{53}$$

These moments lead to random magnetization of the sample and generate a fluctuating B-field. Unlike B^{CP}, this field is not correlated with the direction of the external E-field and it is the main source of the noise. In our case, the signal-to-noise ratio is

$$S/N = 3\frac{\langle \mu_{\text{mol}}^{\text{CP}} \rangle}{\mu_B}\sqrt{\mathcal{N}\frac{t}{\tau}}, \tag{54}$$

where $\mathcal{N}$ is the number of molecules, t is the observation time, and τ is the correlation time for the random thermal magnetization. Factor 3 at the right hand side appears because of the averaging of the magnetic moment (53) over orientations of the molecular axis $\boldsymbol{n}$.

For a strong spin-rotation coupling, as in the case of HgH, τ is determined by interaction of molecular axis with environment. One of such mechanisms is the dipolar interaction between guest radicals, so that $\tau \sim \hbar/(D^2 n) = 4\pi\hbar/(3k_BT)$ for the optimal density (47). For the weak-field limit (51) we get

the final expression for S/N:

$$S/N = \frac{3}{8\pi} \frac{E E_{\text{eff}} d_e}{k_B T} \sqrt{Vt/\hbar}, \qquad (55)$$

where V is the sample volume. This equation is used in Table 6 to estimate accumulation time needed to reproduce the current limit (1). For HgH molecule we find that for a volume of $0.1\,\text{cm}^3$ and strong polarizing field, the present eEDM limit may be recovered within $t = 10^{-6}\,\text{s}$ (3 ms for the field 10 kV/cm). By integrating the signal for one week, the present eEDM limit may be improved by a factor of 2×10^6. Note that these estimates are close to the estimates based on the projected sensitivity to the weak magnetic fields Lamoreaux (2002).

7 Conclusion

In this contribution we developed general formalism for CP-violating polarizability and made estimates for three different systems. The first is liquid Xe, two others include heavy diatomic molecules in a rare-gas matrix. All three systems are supposed to be at a temperature of few Kelvin.

CP-violating polarizability of all systems considered here is described by the third order expressions (26–28). However, the size of the effect is very different. This difference can not be attributed to the Z-scaling, as all three systems have comparable values of Z. The important difference is the nature of intermediate states in the sums (26–28). For a diamagnetic atom, like Xe, both intermediate states are electronic excited states. Consequently, both energy denominators are of the order of a fraction of atomic unit ($10^4 - 10^5\,\text{cm}^{-1}$). For a polar diamagnetic molecule, like BiF, there is non-zero dipole moment of the ground electronic state and one of the intermediate states in the sums (26–28) can be taken to be rotational excited state. Now one of the denominators is of the order of the rotational constant B, typically less than 1 cm^{-1}. On such a small energy scale thermal averaging over rotational states becomes important. As a result, the effective size of the denominator is equal to $k_B T$. That gives us four, or five orders of magnitude enhancement of the effect, compared to atoms. Diamagnetic molecules have zero magnetic moment of the ground state and we need to decouple electron spins in the second intermediate state. Thus, another denominator is still large. Paramagnetic molecules, like HgH, have uncoupled electron spin in the ground electronic state and we can take second intermediate state also to be rotationally excited. Now we have both denominators of the order of the rotational constant B, or of the order of $k_B T$ after averaging over the thermal distribution. That gives us one more enhancement factor of the order of $10^4 - 10^5$. This last enhancement is similar to

the enhancement of the conventional magnetic susceptibility of paramagnetic substances, compared to diamagnetic ones.

We see, that the effect for paramagnetic molecules is about nine orders of magnitude stronger, than for diamagnetic atoms. There is a price to be paid for such an enhancement. First, the density of molecules in a matrix is two, three orders of magnitude smaller, than the density of LXe (according to Eq. (34), the signal is directly proportional to the density). Second, the matrix isolation technique requires smaller sample size. This leads to additional geometrical factor $\gamma \sim 0.1$ and the enhancement becomes $10^5 - 10^6$. Finally, the smaller number of particles in a sample affects S/N ratio. With all these factors included, the overall gain is still huge, and experiment with paramagnetic molecules looks very promising.

It is also interesting to compare this proposal with solid state experiments prepared by Sushkov et al. (2009). Formally, for the solid it is also possible to use (26–28), but realistic calculations are much more difficult (Mukhamed-janov et al. (2003)). For an estimate, though, we can use the same argument as above. For the paramagnetic system one of the intermediate states can be a low energy lattice excitation, but the second electronic polarization requires excited electronic states. Consequently, we end up with one energy denomi-nator of the order of $k_B T$ and another one of the order of 10^4 cm^{-1}. Thus, for the individual paramagnetic center we loose roughly four orders of mag-nitude in enhancement, compared to paramagnetic molecule. In addition we loose one, or two orders of magnitude due to the high orbital angular mo-mentum ($l = 3$) of the unpaired electrons. As a result, an effective electric field felt by the electron in a gadolinium-gallium garnet (GGG) is about 10^5 V/cm (Mukhamedjanov et al. (2003)), compared to 10^{10} V/cm for HgH. On the other hand, the spin density in GGG is 8×10^{22} cm^{-3} about three orders of magnitude higher, than for HgH in a matrix. The sample size for GGG can be also made larger optimizing geometry and improving S/N ratio. We conclude that these two proposed experiments have roughly comparable sensitivity. The advantage of the HgH in a matrix is a much more transparent theory, which allows for a reliable estimate of the β^{CP}.

At the present stage when actual experiments have not started the detailed discussion of the systematic effects is difficult. From the general considerations one can expect that they will be similar to those in the solid state experiments. When the high voltage is applied to the sample the unavoidable leakage cur-rents can cause T-odd spurious effects. In our case such currents are suppressed due to cryogenic temperatures and relatively small electric field, compared to other solid state experiments. In addition, all volume effects are suppressed by the small size of the sample. Therefore, we think that systematic effect for the matrix isolation experiment can be made smaller than in solid state experiments.

To summarize, our proposed eEDM search combines advantages of the strong intermolecular field with a high attainable number density of molecules embedded in a matrix of rare-gas atoms. We argue that our proposal has a potential of improving the present eEDM limit by several orders of magnitude. That will allow constraining the "new physics" beyond the Standard Model at an important new level and, in particular, testing predictions of competing SUSY models.

References

Amini, J. M., Munger, Jr., C. T., Gould, H., 2007. Electron electric-dipole-moment experiment using electric-field quantized slow cesium atoms. Phys. Rev. A 75, 063416.

Amsler, C., et al., 2008. Review of particle physics. Phys. Lett. B 667, 1.

Andrews, L., Moskovits, M. (Eds.), 1989. Chemistry and physics of matrix-isolated species. Elsevier Science, New York, NY, USA.

Barkov, L. M., Zolotorev, M. S., 1978. Pis'ma v ZhETP 27, 379, Sov. Phys. JETP Lett. **27** 357.

Baryshevsky, V. G., 2004. Time-reversal violating generation of static magnetic and electric fields and a problem of EDM measurements. Phys. Rev. Lett. 93, 043003.

Baryshevsky, V. G., Matsukevich, D. N., 2002. Time-reversal-violating rotation of a polarization plane of light in gas placed in an electric field. Phys. Rev. A 66, 062110.

Bickman, S., Hamilton, P., Jiang, Y., Demille, D., 2009. Preparation and detection of states with simultaneous spin alignment and selectable molecular orientation in PbO. Phys. Rev. A 80, 023418.

Bigi, I. I., Sanda, A. I., 2000. CP Violation. Cambridge University Press, Cambridge.

Bouchiat, M. A., Bouchiat, C., 1974. Parity violation induced by weak neutral currents in atomic physics. i. J. Phys. 35 (12), 899–927.

Bouchiat, M.-A., Bouchiat, C., 1997. Parity violation in atoms. Rep. Prog. Phys. 60, 1351–94.

Budker, D., Kimball, D. F., Rochester, S. M., Yashchuk, V. V., Zolotorev, M., 2000. Sensitive magnetometry based on nonlinear magneto-optical rotation. Phys. Rev. A 62 (4), 043403.

Budker, D., Lamoreaux, S. K., Sushkov, A. O., Sushkov, O. P., 2006. Sensitivity of condensed-matter P- and T-violation experiments. Phys. Rev. A 73, 022107.

Budker, D., Romalis, M. V., 2007. Optical magnetometry. Nature Physics 3, 227 – 234.

Bui Dang, H., Romalis, M., 2009. Atomic Magnetometry in the AttoTesla Regime. APS Meeting Abstracts, 3003.

Chin, C., Leiber, V., Vuletic, V., Kerman, A. J., Chu, S., 2001. Measurement of an electron's electric dipole moment using Cs atoms trapped in optical lattices. Phys. Rev. A 63 (3), 033401.

Cho, D., Sangster, K., Hinds, E. A., 1989. Tenfold improvement of limits on t violation in thallium fluoride. Phys. Rev. Lett. 63 (23), 2559–62.

Christenson, J. H., Cronin, J. W., Fitch, V. L., Turlay, R., Jul 1964. Evidence for the 2π decay of the K_2^o meson. Phys. Rev. Lett. 13 (4), 138–140.

Conti, R. S., Khriplovich, I. B., 1992. New limit on T-odd, P-even interactions. Phys. Rev. Lett. 68, 3262–5.

Derevianko, A., Kozlov, M. G., 2005. Molecular CP-violating magnetic moment. Phys. Rev. A 72, 040101(R).

Ernst, W. E., Kandler, J., Torring, T., 1986. Hyperfine structure and electric dipole moment of BaF X^2. J. Chem. Phys. 84, 4769.

Flambaum, V. V., 1976. On EDM enhancement in heavy atoms. Yad. Phys. 24, 383, [Sov. J. Nucl. Phys. 24, 199 (1976)].

Fortson, E. N., Sandars, P., Barr, S., 2003. The search for a permanent electric dipole moment. Physics Today 56(6), 33–39.

Ginges, J. S. M., Flambaum, V. V., 2004. Violations of fundamental symmetries in atoms and tests of unification theories of elementary particles. Phys. Rep. 397, 63.

Griffith, W. C., Swallows, M. D., Loftus, T. H., Romalis, M. V., Heckel, B. R., Fortson, E. N., 2009. ArXiv:0901.2328.

Heidenreich, B. J., et al., 2005. Measurement of the electron electric dipole moment using GdIG. Phys. Rev. Lett. 95, 253004.

Hopkinson, D. A., Baird, P. E. G., 2002. An interferometric test of time reversal invariance in atoms. J. Phys. B 35, 1307–27.

Hudson, J. J., Sauer, B. E., Tarbutt, M. R., Hinds, E. A., 2002. Measurement of the electron EDM using YbF molecules. Phys. Rev. Lett. 89, 023003.

Ignashevich, V. K., 1969. Calculation of enhancement factor for electron edm in nickel-zinc ferrite? Zh. Exper. Teor. Fis. 56, 2019.

Jackson, J. D., 1999. Classical Electrodynamics, 3rd Edition. John Willey & Sons, New York.

Johnson, W. R., 2007. Atomic Structure Theory: Lectures on Atomic Physics. Springer, New York, NY.

Johnson, W. R., Blundell, S. A., Sapirstein, J., 1988. Finite basis sets for the Dirac equation constructed from B–splines. Phys. Rev. A 37 (2), 307–15.

Khriachtchev, L., et al., 2005. IR absorbtion spectrum of matrix isolated noble-gas hydride molecules: Fingerprints of specific interactions and hindered

rotation. J. Chem. Phys. 122, 014510.

Khriplovich, I. B., 1991. Parity non-conservation in atomic phenomena. Gordon and Breach, New York.

Khriplovich, I. B., Lamoreaux, S. K., 1997. CP Violation without Strangeness. Springer, Berlin.

Kiljunen, T., Schmidt, B., Schwentner, N., 2005. Intense-field alignment of molecules confined in octahedral fields. Phys. Rev. Lett. 94 (12), 123003.

Kominis, I. K., Kornack, T. W., Allred, J. C., Romalis, M. V., 2003. A sub-femtotesla multichannel atomic magnetometer. Nature 422, 596–9.

Kozlov, M., Labzowski, L., 1995. Topical review: Parity violation effects in diatomics. J. Phys. B 28, 1933–61.

Kozlov, M. G., 1985. Semiempirical calculation of P- & P,T-odd effects in diatomic molecules. Sov. Phys.–JETP 62, 1114.

Kozlov, M. G., 1997. Enhancement of the electric dipole moment of the electron in the YbF molecule. J. Phys. B 30, L607–12.

Kozlov, M. G., Derevianko, A., 2006. Proposal for a sensitive search for the electric dipole moment of the electron with matrix-isolated radicals. Phys. Rev. Lett. 97, 063001.

Kozlov, M. G., Porsev, S. G., 1989. The possibility to study the break of time-reversal invariance in atoms. Phys. Lett. A 142, 233–6.

Lamoreaux, S. K., 2002. Solid state systems for electron electric dipole moment and other fundamental measurements. Phys. Rev. A 66, 022109.

Landau, 1957. Zh. Eksp. Teor. Fiz. 32, 405, [Sov. Phys. JETP **5**, 405 (1957)].

Landau, L. D., Lifshitz, E. M., 1997. Quantum Mechanics, 3rd Edition. Vol. III. Butterworth-Heinemann.

Moskalev, A. N., 1986. Some macroscopic effects of P- and T-violation in atoms. In: Proc. of the International Symposium on Weak and Electromagnetic Interactions in Nuclei. Springer-Verlag, Berlin, pp. 638–9.

Mukhamedjanov, T. N., Dzuba, V. A., Sushkov, O. P., 2003. Enhancement of the electron electric dipole moment in gadolinium garnets. Phys. Rev. A 68, 042103.

Nayak, M. K., Chaudhuri, R. K., 2008. Calculation of the electron-nucleus scalar-pseudoscalar interaction constant w_s for ybf and baf molecules: A perturbative approach. Phys. Rev. A 78, 012506.

Nedelec, O., Majournat, B., Dufayard, J., 1989. Configuration mixing and line intensities in CdH and HgH $A - X$ transitions. Chem. Phys. 134, 137.

Porsev, S. G., Beloy, K., Derevianko, A., 2009. Precision determination of electroweak coupling from atomic parity violation and implications for particle physics. Phys. Rev. Lett. 102 (18), 181601.
URL http://link.aps.org/abstract/PRL/v102/e181601

Pryor, C., Wilczek, F., 1987. Artificial vacuum for T-violation experiment. Phys. Lett. B 194, 137.

Purcell, E. M., Ramsey, N. F., Jun 1950. On the possibility of electric dipole moments for elementary particles and nuclei. Phys. Rev. 78 (6), 807.

Raidal, M., et al., 2008. Flavour physics of leptons and dipole moments. Eur.

Phys. J. C 57, 13–182.

Ravaine, B., Derevianko, A., 2004. Effects of confinement on the permanent electric-dipole moment of Xe atoms in liquid Xe. Phys. Rev. A 69 (5), 050101(R).

Ravaine, B., Kozlov, M. G., Derevianko, A., 2005. Atomic CP-violating polarizability. Phys. Rev. A 72, 012101.

Regan, B. C., Commins, E. D., Schmidt, C. J., DeMille, D., 2002. New limit on the electron electric dipole moment. Phys. Rev. Lett. 88, 071805.

Ryabov, V. L., Ezhov, V. F., Kartasheva, M. A., 2006. Inductively connected plasma as a new source of molecular beams. Pis'ma v Zh. Tekh. Fiz. 32, No 22, 26.

Sandars, P. G. H., 1965. The electric dipole moment of an atom. Phys. Lett. 14, 194.

Sandars, P. G. H., 1967. Measurability of the proton electric dipole moment. Phys. Rev. Lett. 19, 1396.

Sauer, B. E., Wang, J., Hinds, E. A., 1995. Anomalous spin-rotation coupling in the $\mathbf{X^2}\Sigma^+$ state of YbF. Phys. Rev. Lett. 74, 1554.

Shapiro, F. L., 1968. Electric dipole moments of elementary particles. Sov. Phys. Uspekhi 11, 345.

Stowe, A. C., Knight Jr., L. B., 2002. Electron spin resonance studies of ^{199}HgH, ^{201}HgH, ^{199}HgD and ^{201}HgD isolated in neon and argon matrices at 4K: an electronic structure investigation. Molecular Physics 100, 353.

Sushkov, A. O., Eckel, S., Lamoreaux, S. K., 2009. Prospects for a new search for the electron electric-dipole moment in solid gadolinium-iron-garnet ceramics. Phys. Rev. A 79, 022118.

Sushkov, O. P., Flambaum, V. V., 1978. Parity violation effects in diatomic molecules. Sov. Phys.–JETP 48, 608.

Tarbutt, M. R., Hudson, J. J., Sauer, B. E., Hinds, E. A., 2009. Cold Molecules: Theory, Experiment, Applications. CRC Press, Ch. Prospects for measuring the electric dipole moment of the electron using electrically trapped polar molecules, p. 555, arXiv:0811.2950.

Titov, A. V., Mosyagin, N. S., Ezhov, V. F., 1996. P,T-odd spin-rotational hamiltonian for YbF molecule. Phys. Rev. Lett. 77, 5346–9.

Varentsov, V. L., Gorshkov, V. G., Ezhov, V. F., Kozlov, M. G., Labzovskii, L. N., Fomichev, V. N., 1982. Possible P, T-odd effects in NMR spectroscopy of molecules. Pis'ma Zh. Eksp. Teor. Fiz. 36 (5), 141–4, [JETP Lett. **36** 175 (1982)].

Vasiliev, B. V., Kolycheva, E. V., 1978. Measurement of the electron electric dipole moment using the quantum interferometer. Sov. Phys.–JETP 47, 243.

Weltner, Jr., W., 1990. Magnetic Atoms and Molecules (Dover Books on Physics and Chemistry). Dover Publications.

Wood, C. S., Bennett, S. C., Cho, D., Masterson, B. P., Roberts, J. L., Tanner, C. E., Wieman, C. E., 1997. Measurement of parity nonconservation and an anapole moment in cesium. Science 275, 1759–63.

Wu, C. S., Ambler, E., Hayward, R. W., Hoppes, D. D., Hudson, R. P., 1957.

Experimental test of parity conservation in beta decay. Phys. Rev. 105 (4), 1413–1415.

Zel'dovich, Y. B., 1959. ZhETP 36, 964, Sov. Phys. JETP **9**, 682.